

# **CNWRA** *A center of excellence in earth sciences and engineering*

A Division of Southwest Research Institute™

6220 Culebra Road • San Antonio, Texas, U.S.A. 78228-5166  
(210) 522-5160 • Fax (210) 522-5155

April 25, 2001

Contract No. NRC-02-97-009

Account No. 20.01402.571

U.S. Nuclear Regulatory Commission  
ATTN: Tae Ahn  
Two White Flint North  
11545 Rockville Pike  
Mail Stop T7 C6  
Washington, DC 20555

Subject: Review of revised IM—Effects of Environmental and Metallurgical Conditions on the Passive and Localized Dissolution of Ti-0.15Pd, Intermediate Milestone 01402.571.010

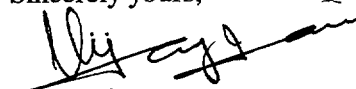
Reference: Letter from T. Ahn to V. Jain, April 12, 2001: Acceptance of Intermediate Milestone 01402.571.010 "Effects of Environmental and Metallurgical Conditions on the Passive and Localized Dissolution of Ti-0.15Pd"

Dear Dr. Ahn:

Please find enclosed a revised version of IM01402.571.010 "Effects of Environmental and Metallurgical Conditions on the Passive and Localized Dissolution of Ti-0.15Pd" that has been modified based on recent NRC comments. Also enclosed is a summary of the responses to NRC comments noting that these have been incorporated into the document. Please advise me of the results of your review, so that we can resubmit the paper for publication in a timely manner.

If you have any questions regarding this paper, please feel free to contact Sean Brossia at (210) 522-5797 or Gustavo Cragnolino at (210) 522-5538.

Sincerely yours,



Vijay Jain  
Element Manager  
Corrosion Science & Process Engineering

BS:NS:jg

Attachment

cc:	J. Linehan	J. Greeves	J. Piconne	B. Leslie	CNWRA EMs
	D. DeMarco	C. Greene	T. Essig	G. Cragnolino	T. Nagy (contracts)
	B. Meehan	T. Bloomer	J. Thomas	W. Patrick	P. Maldonado
	E. Whitt	K. Stablein	J. Andersen	CNWRA Dirs.	



Washington Office • Twinbrook Metro Plaza #210  
12300 Twinbrook Parkway • Rockville, Maryland 20852-1606

- (1) **Clarify on page 8, there are 4 solutions listed in reference to figure 9 that has 3 curves; the paragraph starting with "Also" states 2 dashed lines referenced in figure 9 that has no dashed lines.**

Accept. This has been clarified in the test.

- (2) **In view of the sensitivity of corrosion rates here to the real drip shield (DS) life, delete all corrosion rates (/year) in p.7 (~ 0.7) and p.8 ( $8 \times 10^{-3}$  mm/y and converted to mm/y).**

Accept. All references to corrosion rates in "mm/y" have been removed.

- (3) **In p.3, add a sentence about why these solutions were chosen for these DS tests.**

Clarification that the solutions used were not "mixed anion" solutions and that "mixed anion" solutions will be evaluated in future work has been made.

- (4) **Explain the implication in the DS life about (a) that the location of corrosion attack was concentrated at the weldments for welded specimens (p. 6); (b) welds did act as preferential sites for localized corrosion initiation (p. 11); and (c) the top paragraph (p. 13).**

Accept. Clarification that the effects of weldments on DS life expectancy may need to be evaluated further has been added.

- (5) **In CONCLUSION, (a) specify actual test solutions in presenting corrosion test results and address the welded specimen in terms of corrosion attack.**

Accept. The conclusions have been clarified to reflect that simple chloride and chloride + fluoride solutions were used in this work and that more extensive attack was observed at the weldments.

EFFECTS OF ENVIRONMENTAL AND METALLURGICAL CONDITIONS ON THE  
PASSIVE AND LOCALIZED DISSOLUTION OF Ti-0.15Pd

C.S. Brossia and G.A. Cragolino

Center for Nuclear Waste Regulatory Analyses

Southwest Research Institute

6220 Culebra Road

San Antonio, TX 78238

ABSTRACT

The effects of chloride concentration, fluoride concentration, pH, temperature, and weldments on the corrosion behavior of Ti-0.15Pd (Ti Grade 7, UNS R52400) were examined. It was noted that even at elevated temperatures (165 °C), the passivity breakdown and repassivation potentials were well above 1 V<sub>SCE</sub> in solutions containing 4 M Cl<sup>-</sup>. It was also observed that welded specimens exhibited lower breakdown and repassivation potentials than wrought specimens. Short-term anodic polarization tests revealed that chloride concentration, pH, and applied potential had only a slight effect on passive current density of Ti Grade 7. Fluoride additions to chloride solutions resulted in the appearance of a pseudo active/passive transition and a significant increase in the potential-independent anodic current density, that was several orders of magnitude greater than typical passive current densities. Also of note was the observation that despite the use of creviced specimens, all corrosion attack took place on the boldly

exposed surfaces of the specimens.

Keywords: titanium, titanium palladium alloys, localized corrosion, weldments, fluoride, chloride

## INTRODUCTION

The safety strategy adopted by the U.S. Department of Energy (DOE) for the proposed high-level nuclear waste (HLW) repository at Yucca Mountain (YM) relies on several key attributes for the unsaturated repository system, one of which is the integrity of the drip shield (DS) to divert incoming water away from the waste packages.<sup>1</sup> Primary materials being considered by the DOE for construction of the drip shield are Pd-bearing Ti alloys, such as Ti Grade 7<sup>a</sup> (UNS R52400) and Ti Grade 16<sup>b</sup> (no UNS designation). Ti-Pd alloys are  $\alpha$  Ti alloys that have similar mechanical properties to commercial purity (CP) Ti, but exhibit considerably better corrosion resistance than CP Ti in many aqueous environments.<sup>2</sup>

Ti alloys are known to exhibit excellent corrosion resistance under many conditions as a result of the spontaneous formation of a protective TiO<sub>2</sub> passive film. Under undisturbed repository conditions, precipitation of salts from minerals and constituents found in the prevailing groundwater at YM may occur when incoming water contacts the heated DS surface that may in turn lead to enhanced corrosion. Studies have shown that the concentration of aggressive species such as chloride (Cl<sup>-</sup>)<sup>3</sup> and fluoride (F<sup>-</sup>)<sup>4</sup> can reach concentrations as high as 5 and 0.2 M, respectively, when simulated groundwater chemistries are subjected to evaporative concentration processes. Additional studies have also shown that liquid water containing entrained solids can penetrate a boiling isotherm<sup>5</sup>, thus the possibility exists that at the elevated temperatures

---

<sup>a</sup>Nominal Composition (max wt%): 0.03 N, 0.10 C, 0.015 H, 0.30 Fe, 0.25 O, 0.12–0.25 Pd, bal. Ti.

<sup>b</sup>Nominal Composition (max wt%): 0.03 N, 0.10 C, 0.015 H, 0.30 Fe, 0.25 O, 0.05 Pd, bal. Ti.

resulting from radioactive decay a highly concentrated solution may contact the DS. Furthermore, the DS will be fabricated though the use of weldments that also may influence material performance. Thus, the goal of this study was to examine the effects of environmental variables (temperature,  $\text{Cl}^-$  concentration,  $\text{F}^-$  concentration) and weldments on the corrosion behavior of Ti Grade 7. In particular, emphasis was placed on the effects of these variables on the passive current density and on localized corrosion susceptibility in the form of critical potentials [i.e., breakdown potential ( $E_{\text{bd}}$ ) and repassivation potential ( $E_{\text{rp}}$ )] as these parameters have been demonstrated as being useful to predict long-term material performance<sup>2</sup>.

## EXPERIMENTAL APPROACH

All tests were performed using specimens machined from a 2.5-cm thick plate from a single heat of Ti Grade 7, the chemical composition of which is shown in Table 1. Specimens were machined in the form of cylinders 6.3 mm in diameter and 48.6 mm in length or as standard crevice specimens in the form of blocks with dimensions of  $19 \times 19 \times 12$  mm (length  $\times$  width  $\times$  thickness) with an 8-mm hole through the thickness to facilitate attachment of the crevice former. For crevice specimens, a serrated polytetrafluoroethylene (PTFE) crevice former having 12 crevice feet was used and pressed against the flat portion of the specimen at a torque of 0.28 N·m. In the case of welded crevice specimens, the plate was cut into 1.25 cm thick sections and welded together using 10 passes per side. The composition of the weld wire used and the resulting weldment are also shown in Table 1. All specimens were wet polished to a 600 grit finish and ultrasonically cleaned in acetone and water prior to testing. All test solutions were made from reagent grade sodium salts, reagent grade acids and 18 M $\Omega$ ·cm water without including other anions present on the groundwater (e.g., sulfate, carbonate). The effects of these anions on the corrosion behavior

of Ti will be evaluated in future studies. For tests conducted in glass cells, after the bulk solution was made, the solution was introduced into the test cell, purged with high purity N<sub>2</sub> and the solution was heated to the desired temperature prior to introduction of the specimen to the cell. All tests used a Pt-coated Nb mesh counter electrode and a saturated calomel electrode (SCE) as a reference, connected into the cell through a salt bridge/Luggin probe to maintain the reference electrode at room temperature. No correction for the liquid thermal junction potential was made and is not included in the reported potentials herein.

In the case of tests conducted at temperatures greater than 100 °C, a PTFE-lined type 316L (UNS 531603) autoclave was used. In the autoclave tests, the solution and specimen were introduced simultaneously, then the solution was purged with high purity N<sub>2</sub> and heated to the desired temperature in the range from 95 to 165 °C prior to testing. Tests were conducted at 95 °C to serve as a basis for comparison of the autoclave results to the results observed from testing in the glass cells. A Pt-coated Nb mesh was used as a counter electrode and an internal Ag/AgCl (0.1 M KCl) reference electrode, similar to that discussed by Macdonald et al.<sup>6,7</sup> and reviewed by Cragolino,<sup>8</sup> was used. All potentials shown from autoclave tests are reported versus SCE at 25 °C, using the conversions provided by Cobble.<sup>9</sup>

Both cyclic potentiodynamic and potentiostatic polarization tests were performed. Cyclic polarization tests were performed at a scan rate of 0.167 mV/s and were reversed at a current density of 5 mA/cm<sup>2</sup> with the exception of tests conducted in fluoride solutions, in which case the scans were reversed at 1.0 V<sub>SCE</sub>. Potentiostatic tests were performed to examine environmental effects on passive dissolution and to examine the effects of long-term polarization on the possible initiation of localized corrosion.

## EXPERIMENTAL RESULTS

Figure 1 shows a typical polarization curve for this material in chloride only solutions, with high breakdown ( $E_{bd}$ ) and repassivation ( $E_{rp}$ ) potentials evident. Figure 2 summarizes the effects of chloride concentration and weldments on  $E_{bd}$  and  $E_{rp}$  determined from cyclic potentiodynamic polarization experiments performed at 95 °C. The typical attack morphology observed after polarization is shown in Figure 3. Note the irregular nature of the attack and some evidence of undercutting, resulting from the spread of the attack underneath the oxide film. Furthermore, under no conditions was attack observed under the crevice former, but rather all attack was observed on the boldly exposed surfaces of the specimens. As a result, the breakdown and repassivation potentials labeled in Figure 1 as  $E_{bd}$  and  $E_{rp}$  are not crevice and crevice repassivation potentials but are associated with the boldly exposed surface. Though the presence of weldments appeared to be slightly detrimental, when examined in the context of the variability (shown by the error bars) of  $E_{bd}$  and  $E_{rp}$  there is little difference between the wrought and the welded material. Consequently, Eq. 1 was fit to both sets of data (wrought and welded),

$$E_{crit} = E_{crit}^0 - B \log[Cl^-] \quad (1)$$

where  $E_{crit}$  is the critical potential (either  $E_{bd}$  or  $E_{rp}$ ),  $E_{crit}^0$  is the critical potential at 1 M chloride concentration, and  $B$  is the slope of the dependence of  $E_{crit}$  on the log of the chloride concentration. For  $E_{bd}$ , the slope was found to be approximately 2.28 V/decade·[Cl<sup>-</sup>] with  $E_{bd}^0$  at 7.30 V<sub>SCE</sub> and an  $r^2$  of 0.92. For  $E_{rp}$ , the slope was 0.67 V/decade·[Cl<sup>-</sup>] with an  $E_{rp}^0$  of 5.64 V<sub>SCE</sub> and  $r^2$  of 0.84. Slightly better fitting results were obtained for  $E_{rp}$  when the wrought and welded data sets were examined independently ( $r^2$  increased to 0.96 for both  $E_{bd}$  and  $E_{rp}$  for the wrought material), however, given the overlapping

variability ranges for most of the data sets, they were examined as a single set. Even though the critical potentials for the welded and wrought materials were very similar, it should be noted that the location of corrosion attack was more extensive at the weldments for welded specimens. Furthermore, long-term (up to 6 weeks) potentiostatic polarization tests at potentials as high as  $1.5 V_{SCE}$  did not result in any observable localized corrosion of Ti even in high chloride solutions, and negligible weight change was measured<sup>c</sup>. This indicated that the specimen was passive throughout the testing period.

The effect of temperature on  $E_{bd}$  and  $E_{tp}$  for both wrought and welded specimens in 1 M and 4 M chloride is shown in Figures 4 and 5. As was observed at 95 °C, the welded specimens exhibited slightly lower critical potentials than did the wrought specimens. Further, increases in temperature resulted in a linear decrease in the critical potentials up to a certain point, then an abrupt decrease was observed, followed by a continued linear decrease with increasing temperatures. The critical temperature ( $T_{crit}$ ) at which this abrupt decrease was observed was between 140 and 165 °C for  $E_{bd}$  and between 120 and 140 °C for  $E_{tp}$ . Again, however, the critical potentials observed were well above  $1 V_{SCE}$ , with the lowest observed  $E_{tp}$  being  $1.23 V_{SCE}$  for welded Ti Grade 7 at 165 °C. When exposed to 4 M chloride solutions, similar results were observed with only a shift towards lower potentials (as would be expected) noted. Furthermore, even at 165 °C in 4 M chloride,  $E_{tp}$  was still above  $1 V_{SCE}$ .

To evaluate the passive behavior of Ti Grade 7 and the potential influences of environment on the rate of passive dissolution, a series of short-term (~ 24 h) potentiostatic experiments were performed. The results of these experiments are shown in Figures 6 and 7. Figure 6 shows the effects of applied potential

---

<sup>c</sup>Minimum, accurate weight change measurable was 0.05 mg, which roughly corresponds to a corrosion rate of  $10^{-3}$  mm/yr for Ti Grade 7.



on the passive current density measured in two different chloride solutions, 1 and 0.1 M (pH ~ 6.5), at 95 °C. Little effect of applied potential on the passive current density was observed. For example, in 0.1 M NaCl the passive current density at  $-0.25 V_{SCE}$  was  $2.5 \mu A/cm^2$  whereas at  $+0.50 V_{SCE}$  it was  $5.4 \mu A/cm^2$ . At  $-0.25 V_{SCE}$ , increasing the chloride concentration from 0.1 to 1 M resulted in an increase in the passive current density from  $2.5 \mu A/cm^2$  to  $18.2 \mu A/cm^2$ . Error bars in Figures 6 and 7 represent the range of values observed through out the length of the test. Figure 7 shows the effects of applied potential and pH on passive dissolution in 1 M chloride at 95 °C. Both increases in the pH from 6.5 to 10.5 and decreases in the pH to 2.1 generally resulted in a decrease in the passive current density, especially at higher applied potentials. For example, at an applied potential of  $0 V_{SCE}$ , the passive current density at pH 6.5 was nearly  $30 \mu A/cm^2$ . By increasing the pH to 10.5 or decreasing the pH to 2.1, the passive current density decreased to 7.1 and  $1.7 \mu A/cm^2$ , respectively. Greater variability in the measured passive current density was also observed in both alkaline and acidic solutions compared to neutral solutions.

To confirm the results obtained and examine the effects of long-term polarization on the passive current density, an additional series of potentiostatic tests were performed. In general it was observed that the initial passive currents were high, but then decreased and eventually reached a steady state after about 100 h. Figure 8 shows the results from a potentiostatic hold of Ti Grade 7 in deaerated 1 M chloride at 95 °C and an applied potential of  $+0.0 V_{SCE}$ . After an initial period of relatively rapid dissolution, the current density decreased to nearly constant values approaching  $8 \times 10^{-8} A/cm^2$  after 150 h.

In addition to the likely presence of chloride in the proposed repository, the possibility exists for fluoride to also be present as it is known to exist in the local groundwater at YM. Thus, the effect of fluoride on the polarization of Ti Grade 7 was examined. Shown in Figure 9 are three polarization curves for non-

creviced specimens comparing the anodic behavior observed in 1 M NaCl, 1 M NaF, and 1 M NaF + 1 M NaCl. Ti Grade 7 exhibited a considerably lower open circuit potential in all solutions containing fluoride and a pseudo active/passive transition with a subsequent potential independent current region with current densities considerably higher than those typically encountered during passive dissolution ( $10^{-3}$  to  $10^{-1}$  as compared to  $\sim 10^{-6}$  A/cm<sup>2</sup>). It is also interesting to note that in the non-acidified fluoride solutions there existed a small area of passivity just noble of the open circuit potential, prior to a sharp increase in the current (similar to what is observed during localized corrosion) which then decreased after reaching a critical current density. Post-test examination of the specimens revealed extensive attack, but the attack was general.

Also noted in Figure 9 are solid horizontal lines which represent the range of steady state open circuit potentials for Ti measured in chloride solutions under air-saturated conditions (from -0.3 to 0 V<sub>SCE</sub>).<sup>10</sup> Using the maximum observed potential ( $\sim 0$  V<sub>SCE</sub>) as a reference point of comparison, the current density observed as a function of fluoride concentration was examined. Shown in Figure 10 is the current density in A/cm<sup>2</sup> observed at 0 V<sub>SCE</sub> as a function of fluoride concentration for both wrought and welded Ti in 1 M chloride solutions. Also shown is the current density observed for wrought material in 0.1 M chloride. For comparison, the current density observed at 0 V<sub>SCE</sub> in 1 M chloride is also noted by the horizontal dashed line at 0.7  $\mu$ A/cm<sup>2</sup>. Changes in the chloride concentration and the presence of weldments did not significantly effect the observed current density. Of importance, however, is that there seems to be a critical fluoride concentration below which only a slight elevation in the current density compared to chloride only solutions is observed and above which much higher current densities are seen. This critical fluoride concentration ( $[F^-]_{crit}$ ) seems to be on the order of 0.05 to 0.1 M. Below  $[F^-]_{crit}$ , the current

density was at most one order of magnitude larger than what was observed in chloride only solutions. Above  $[F^-]_{crit}$  a marked increase to current density some three orders of magnitude greater were seen. In addition, when creviced specimens were polarized in these solutions, in contrast to chloride-only solutions, corrosion under the crevice former was observed.

## DISCUSSION

### Localized Corrosion in Chloride Solutions

Based on the results obtained from potentiodynamic polarization, it is clear that  $E_{bd}$  and  $E_{tp}$  for Ti Grade 7 are dependent on the chloride concentration, following the well recognized linear decrease with the logarithm of chloride concentration shown in Eq. 1. In the present work, a slope,  $B$ , of nearly 2.28 V/decade $\cdot[Cl^-]$  was observed for  $E_{bd}$  (Figure 2) for a chloride concentration range of 0.1 to 5 M at 95 °C. These values are considerably larger than those summarized previously by Smialowska<sup>11</sup> of 0.11 V/decade for Ti alloys in bromide solutions and 0.1 V/decade in chloride solutions at 200 °C.<sup>12</sup> It should be noted, though, that the dependence of  $E_{bd}$  on chloride concentration for Pd-bearing Ti alloys has not been previously examined, with the majority of the work similar to this being conducted in other halide solutions.  $E_{tp}$  followed a similar relationship to chloride concentration, but the slope of the logarithmic dependence was lower (0.67 V/decade $\cdot[Cl^-]$ ).

Previous work examining other materials (e.g., nickel based alloys and stainless steels) has shown that the repassivation potential can be used successfully in life prediction calculations.<sup>13,14</sup> In such calculations, the corrosion potential is determined based on cathodic kinetics and the passive current density of the material. This is then compared to the calculated repassivation potential that is determined

at each time step in terms of the predicted temperature and predicted chloride concentration. In the present case, such calculations should show that the repassivation potential for Ti Grade 7 is above the water oxidation potential and, thus, no localized corrosion would be predicted. Simulations of the long-term behavior of Ti Grade 7 resulted in the observation of Ti failures by passive dissolution and no failures by localized corrosion.

Because the proposed repository will be above boiling for some time and because it has been shown that aqueous films may exist well above 100 °C in the presence of deposited salts by forming saturated solutions, the effect of elevated temperatures on the critical potentials for localized corrosion was also examined. Increasing the temperature also resulted in a decrease in the measured critical potentials for Ti Grade 7 (Figures 4 and 5) up to a certain critical temperature,  $T_{crit}$ , above which an abrupt decrease in the critical potentials was observed. At temperatures less than  $T_{crit}$ ,  $E_{bd}$  and  $E_{rp}$  had temperature dependencies ranging from 20 to 33 mV/°C and 11 to 14 mV/°C for the wrought and welded specimens. The critical temperatures observed in the present case (between 140 and 165 °C for  $E_{bd}$  and between 120 and 140 °C for  $E_{rp}$ ) are similar to the value of approximately 125 °C for  $E_{bd}$  in 1 M chloride reported by Posey and Bohlmann<sup>15</sup> for Ti Grade 7. It should be noted, however, that Posey and Bohlmann<sup>15</sup> observed a much stronger temperature dependence for  $E_{bd}$  at temperatures less than  $T_{crit}$  (approximately 70 mV/°C), but similar dependencies at temperatures above  $T_{crit}$ . The source of the differences is unclear, except that Posey and Bohlmann<sup>15</sup> examined the effect of temperature over a wider range than was used in the present study (minimum temperature by Posey and Bohlmann was 25 °C as opposed to the minimum of 95 °C examined here). At  $T_{crit}$  both  $E_{bd}$  and  $E_{rp}$  decrease significantly, by as much as 2.6 V<sub>SCE</sub>, similar to that observed by Posey and Bohlmann.

Similar results were observed with regard to tests conducted in 4 M chloride solutions. In all cases, however,  $E_{tp}$  was again observed to be greater than 1  $V_{SCE}$ , even at 165 °C. This further highlights that localized corrosion of this material under anticipated conditions at the proposed repository in chloride only solutions is unlikely.

Though not discussed in any detail thus far, the effect of welding on the localized corrosion resistance of Ti Grade 7 appears to be somewhat detrimental, though generally within the data scatter observed. It is thought, however, that if a statistically significant number of experiments were conducted under identical conditions that welded Ti Grade 7 would likely exhibit depressed critical potentials compared to wrought Ti Grade 7. But according to Donachie<sup>16</sup> and Schutz,<sup>17</sup> Ti weldments should have comparable corrosion resistance to the wrought material as the formation, structure and thickness of the  $TiO_2$  passive film should be essentially independent of substrate microstructure. In the present case, however, this was not strictly observed and weldments did act as preferential sites for localized corrosion initiation. At first, one could argue that this observation was a consequence of Pd dilution within the weld bead. The composition of the weld wire and the weldment itself, though, seems to counter argue this point in that they were in fact slightly enriched with Pd compared to the base metal. Though not examined in any detail, it seems more likely that the reason for the observed detrimental effects of weldments is a result of differences in the grain structure of the weldment and the heat affected zones as compared to the base metal and possibly through an increased density number of defects at these locations. Another possibility is segregation of Pd in the dendrites or interdendritic regions of the weldment. These possibilities should be evaluated further to determine if welding and subsequent post-weld annealing significantly alter the life expectancy of a Ti DS.

Previous results obtained indicated that a maximum corrosion potential ( $E_{\text{corr}}$ ) on the order of between  $-0.3$  and  $0$   $V_{\text{SCE}}$  is attainable, which is considerably below the repassivation potentials observed for Ti Grade 7.<sup>10</sup> Furthermore, it seems unlikely that potentials outside the region of water stability are possible. The exception to this would be the possible formation of hydrogen peroxide ( $\text{H}_2\text{O}_2$ ) through radiolysis. Neglecting the well known complexation ability of peroxide with Ti for the moment,<sup>18</sup> addition of peroxide would not likely result in  $E_{\text{corr}}$  exceeding the repassivation potential of Ti Grade 7, except in highly concentrated  $\text{H}_2\text{O}_2$  solutions at low pH. For example, at pH 0 and 1 M  $\text{H}_2\text{O}_2$ , the maximum attainable potential without oxidation of peroxide according to thermodynamic calculations<sup>19</sup> is roughly 1.6  $V_{\text{SCE}}$ . Given the unlikelihood of achieving this high concentration of peroxide<sup>20</sup>, this low pH, and the fact that the minimum temperature where this value would exceed the repassivation potential is 140 °C, it does not seem likely that localized corrosion of Ti Grade 7 would occur under repository conditions in chloride-only solutions.

Though it seems that localized corrosion of Ti Grade 7 will only occur under high overpotential conditions in chloride solutions, it was also observed that no corrosion was observed to occur under the PTFE crevice former. This is surprising given that Ti alloys have historically been considered more susceptible to crevice corrosion than to pitting corrosion. One possible explanation for this observation stems from IR drop in the crevice and the diffusion of chloride to the active site. According to Beck,<sup>21</sup> Ti undergoes active dissolution during crevice corrosion as well as at the pit base. In pitting (at high overpotential), the ohmic drop needed to place the pit base in the active region of the polarization curve occurs as a result of a salt film. In crevice corrosion (low overpotential) such a salt film is not needed. Furthermore, according to the experimental work conducted by Beck<sup>21</sup> and Cotton<sup>22</sup>, the rate determining

step for pitting of Ti is the diffusion of chloride to the pit base. Considering now a case where a high overpotential is being applied to the material, IR drop into the crevice will only be sufficient to decrease the potential a few hundred millivolts, not the several volt drop needed to obtain active dissolution, thus passivity is maintained. If chloride diffusion is the rate determining step, then pits will more easily form and propagate outside the crevice as the diffusion distance for chloride is shorter outside. This would then imply that during short term tests, pitting would occur on the outer surfaces and the crevice would remain passive (as was observed). If polarization at high overpotentials were to be conducted for sufficiently long time, then it seems likely that eventually attack under the crevice former would ensue.

#### Passive Dissolution in Chloride Solutions

As a result of the unlikelihood of achieving conditions for localized corrosion of freely corroding Ti Grade 7 in chloride-only solutions, the effects of environmental and electrochemical conditions on passive dissolution were examined. Initial work focused on examining the effects of chloride concentration, pH, and applied potential through short-term potentiostatic tests. In general, increased chloride concentrations from 0.1 to 1 M resulted in an increase in the passive current density, whereas acidification or alkalinization of the solution tended to decrease the passive current density (Figures 6 and 7). Applied potential generally had a minor effect on passive dissolution, as would be expected given that over the potential range examined the thermodynamically stable species is  $\text{TiO}_2$ .<sup>23</sup>

Increases in the chloride concentration did result in a slight increase in the measured current density. In all cases, though, the increase was less than a factor of 7 and at an applied potential of +0.25 V<sub>SCE</sub> the difference was only a factor of 2. The precise reasoning for the slight increase in passive dissolution with

increased chloride concentration is unclear. Work on pure Ti thin films has shown that changes in chloride concentration had little to no effect on the passive current density.<sup>24</sup> Furthermore, extensive industrial experience with Ti in geothermal and desalination applications has not revealed any significant effects of chloride concentration on the passive dissolution of Ti alloys.<sup>25</sup> It seems likely that the observed increases in the present study could very well be a consequence of the short experimental times used (24 hr/test). In addition, considering the variability observed during the pseudo steady-state period of these tests, the relative differences decrease to less than a factor of 3 and in some cases no difference was observed. Thus, the observation that chloride concentration influences the passive current density of Ti Grade 7 may originate in the experimental approach taken.

Changes in the pH tended to have a slight decreasing effect on the passive current density, especially at higher applied potentials. This may indicate a slight enhancement in the stability of the passive film. Examination of the Ti-H<sub>2</sub>O potential-pH diagram,<sup>23</sup> however, does not show that any changes would be expected as the thermodynamically stable species over the range of applied potentials and pH values examined here. As was the case for the effect of chloride concentration, though, the differences observed here, especially when the variability in the measured passive current density is taken into consideration, are relatively small (only between 2 and 8 at a maximum at 0 V<sub>SCE</sub>). Considering these small differences, the observed effect of pH may also be a consequence of the short experimental times used. Furthermore, others have similarly observed that pH exhibited no or only a slight influence on the passive current density of Ti alloys. For example, the passive current density of Ti-15V-3Cr was found to only change by a factor of 2 on decreasing the pH from near neutral to 1.<sup>26</sup> Other work by these authors on pure Ti thin films revealed that pH had no effect on passive current density.<sup>24</sup> Longer-term potentiostatic polarization tests



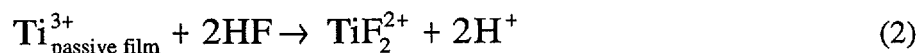
(Figure 8), however, revealed that the high currents observed in the short-term tests were not sustainable. After about 150 h, the current measured had decreased from  $\sim 3 \mu\text{A}/\text{cm}^2$  to  $\sim 0.08 \mu\text{A}/\text{cm}^2$ .

#### Effect of Fluoride on Corrosion Behavior

Another environmental variable to consider with respect to the corrosion behavior of Ti Grade 7 in the proposed repository is the presence of fluoride. Fluoride is present in the local ground water chemistry at levels approaching 0.1 mM.<sup>27</sup> Work examining the possibility of concentration effects through repeated evaporation and re-wetting cycles has estimated that this concentration can increase to at least 0.2 M in the presence of crushed tuff.<sup>4</sup> Though it is known that fluoride acts as a complexant for Ti, the typical concentration ranges that have been examined have been generally in the mM range.<sup>28,29</sup> In addition, there is little information on the effects of higher fluoride concentrations on the corrosion behavior of Pd-bearing Ti alloys, thus this was examined.

In both the 1 M fluoride solution and the fluoride-chloride solution an initial passive region was observed prior to a current increase similar to that which is associated with a passivity breakdown potential for the initiation of localized corrosion. Under all conditions studied, though, general dissolution of the specimens was observed. Thus, the current increase observed after the initial passive region in fluoride solutions is not associated with the initiation of localized corrosion. Rather, further increases in the potential for fluoride solutions resulted in the attainment of a critical current density (peak current density) after which increases in the potential resulted in decreases in the current density, similar to an active/passive transition. A peak current density of approximately  $0.1 \text{ A}/\text{cm}^2$  was observed in all solutions. The potential-independent current density at higher potentials in these solutions ranged from  $10^{-3}$  to  $0.1 \text{ A}/\text{cm}^2$ , which

is considerably higher than the passive current density observed in chloride-only solutions. Furthermore, given the magnitude of these currents, the anodic behavior in this potential region likely is not truly passive. It is possible that these high current densities are limited by transport of  $\text{TiF}_6^{2-}$  through a porous corrosion layer on the surface, similar to the mass transport conditions encountered in electropolishing. Another possibility, which has been proposed in the literature for this apparent mass transport limited dissolution region,<sup>30–32</sup> is the transport of HF to the metal surface as a rate determining step in the reaction sequence shown in Eq. 2,



In any event, it is clear that the presence of fluoride above a critical concentration resulted in marked changes in polarization behavior and current density.

Examination of the effect of fluoride concentration on the current density at a constant potential (Figure 10) revealed that there existed a critical fluoride concentration above which the increase in current density compared to chloride-only solutions was significant. The existence of a critical fluoride concentration is in agreement with what has been observed by others and in some cases is comparable. Boere,<sup>33</sup> for example, observed a decrease in the polarization resistance of CP-Ti in 0.2 M NaCl by a factor of over 30 when the fluoride concentration was increased from 10 mM to 30 mM, in agreement with the nearly two order of magnitude increase in the current density observed in the present work when the fluoride concentration was above 50 mM. In cases where acidified solutions were utilized, the critical fluoride concentration tended to be lower. It seems in the present case, then, that the higher critical fluoride concentration necessary as compared to acidified solutions has to do with the formation of HF in the



solution via Eq. 3,

and enhanced HF production at the dissolving Ti surface when  $\text{H}^+$  is produced from Eq. 2 and reacts with free  $\text{F}^-$  to form HF via Eq. 3 as proposed by Mandry and Rosenblatt.<sup>32</sup> In any event, it is clear that fluoride has a detrimental role on the corrosion behavior of Ti Grade 7.

Also of importance was the observation that limited attack under the crevice former was also observed for Ti Grade 7 in fluoride solutions which exhibited a pseudo active passive transition. Though not all of the corrosion attack was located under the crevice former, this occurrence is a distinguishing feature compared to the results observed in chloride only solutions. Crevice corrosion, in this case, seems to be a result of the added mass transport limitation provided by the crevice former allowing an increased buildup of HF via Eq. 3 and further exacerbated by hydrolysis of Ti cations which are similarly constrained by the crevice former. That localized corrosion of Ti Grade 7 in the form of crevice corrosion is observed in the presence of fluoride at reasonably attainable potentials may indicate that crevice corrosion may be possible in such mixed fluoride-chloride systems under repository conditions. This then suggests that further examination of the long-term effects of fluoride on Ti be examined as well as the possibility of monitoring the fluoride concentration of incoming ground water at the emplacement drifts.

## CONCLUSIONS

Based on the work conducted to date in simple chloride and chloride + fluoride solutions, it seems unlikely that Ti Grade 7 will experience pitting corrosion under anticipated repository conditions. Welded specimens of Ti Grade 7 did exhibit a slight decrease in resistance to pitting compared to wrought

specimens as evidenced by slightly more extensive corrosion attack at the weldments. In all cases for chloride-only solutions, no attack was observed under the crevice former. It is speculated that at high overpotentials and short times localized corrosion is favored on the boldly exposed surfaces rather than occluded regions but if given sufficient time then corrosion attack would also occur in the occluded regions as well. Short term potentiostatic tests did not reveal any significant effects of chloride concentration, pH, or applied potential on the passive current density. Long-term potentiostatic tests also demonstrated that the passive current densities measured during short-term testing were not sustainable nor representative and tended to be ~40x smaller. Lastly, fluoride was noted to strongly alter the anodic polarization behavior of Ti Grade 7 leading to significantly higher currents and in some cases the observation of corrosion attack under the crevice former.

#### ACKNOWLEDGMENTS

The authors would like to acknowledge the financial support of the U.S. Nuclear Regulatory Commission (NRC), Office of Nuclear Material Safety and Safeguards, Division of Waste Management under contract No. NRC-02-97-009 in performing this work. The views presented herein are an independent product of the authors and the Center for Nuclear Waste Regulatory Analyses (CNWRA) and do not necessarily reflect the regulatory position of the NRC. Technical assistance provided by Mr. S. Clay, Mr. J. Spencer and Ms. F. Daby (Southwest Research Institute) for some of the experimental work and SEM microscopy are gratefully acknowledged.

#### REFERENCES

1. Civilian Radioactive Waste Management System Management and Operating Contractor, Repository Safety Strategy: Plan to Prepare the Postclosure Safety Case to Support Yucca Mountain Site Recommendation and Licensing Considerations, TDR-WIS-/RL-000001, Rev. 3, Las Vegas, NV: TRW Environmental Safety Systems, Inc. (2000).

2. G.A. Cragolino, D.S. Dunn, C.S. Brossia, V. Jain, and K.S. Chan, Assessment of Performance Issues Related to Alternate Engineered Barrier System Materials and Design Options, CNWRA 99-003, San Antonio, TX: Center for Nuclear Waste Regulatory Analyses (1999).
3. Civilian Radioactive Waste Management System Management and Operating Contractor, Waste Package Degradation Process Model Report, TDR-WIS-MD-000002, Rev. 00, ICN 01, Las Vegas, NV: TRW Environmental Safety Systems, Inc. (2000).
4. Civilian Radioactive Waste Management System Management and Operating Contractor, Review of the Expected Behavior of Alpha Titanium Alloys Under Yucca Mountain Conditions, TDR-WIS-MD-000015, Rev. 00, Las Vegas, NV: TRW Environmental Safety Systems, Inc. (2000).
5. R.T. Green and J.D. Prikryl, Penetration of the Boiling Isotherm by Flow Down a Fracture, Proceedings of the Third International Symposium on Multiphase Flow, Lyon, France: Technomic Publishing Company (1998).
6. D.D. Macdonald, Modern Aspects in Electrochemistry no. 11, 141 (1975).
7. D.D. Macdonald, J. Pang, C. Lui, E. Medina, J. Villa, and J. Bueno, in Corrosion Control for Low-Cost Reliability, Proceedings 12<sup>th</sup> International Corrosion Congress, 4274, Houston, TX: NACE International (1993).
8. G. Cragolino, in Advances in Localized Corrosion, NACE-9, 413, Houston, TX: NACE International (1987).
9. J.W. Cobble, Journal of the American Chemical Society, 86, 5394 (1964).
10. C.S. Brossia and G.A. Cragolino, Effects of Environmental, Electrochemical, and Metallurgical Variables on the Passive and Localized Dissolution of Ti Grade 7, Corrosion2000, Paper no. 211 Houston, TX: NACE International (2000).
11. Z. Szklarska-Smailowska, Pitting Corrosion of Metals, Houston, TX: NACE International (1986).
12. T. Koizumi and S. Furuya, in Titanium Science and Technology vol. 4., 2383 (1973).
13. D.S. Dunn, G.A. Cragolino, and N. Sridhar, Corrosion, 56, 90 (2000).
14. G.A. Cragolino, S. Mohanty, D.S. Dunn, N. Sridhar, and T. Ahn, Nuclear Engineering and Design, 201, 289 (2000).
15. F.A. Posey and E.G. Bohlmann, Desalination, 3, 269 (1967).

16. M.J. Donachie, *Titanium: A Technical Guide*, Materials Park, OH: ASM International (1988).
17. R.W. Schutz, *Materials Performance*, January 1991, 58 (1991).
18. F.A. Cotton and G. Wilkinson, *Advanced Inorganic Chemistry*, New York, NY: John Wiley & Sons (1980).
19. M. Pourbaix, *Atlas of Electrochemical Equilibria in Aqueous Solutions*, Houston, TX: NACE International (1974).
20. L. Yang, personal communication (2001).
21. T.R. Beck, in *Localized Corrosion*, NACE-3, 644, Houston, TX: NACE International (1974).
22. J.B. Cotton, in *Localized Corrosion*, NACE-3, 676, Houston, TX: NACE International (1974).
23. J.B. Lee, *Corrosion*, 37, 467 (1981).
24. D.G. Kolman and J.R. Scully, *Journal of the Electrochemical Society*, 143, 1847 (1996).
25. M. Conover, P. Ellis, and A. Curzon, in *Geothermal Scaling and Corrosion*, ASTM STP 717. Philadelphia, PA: American Society for Testing and Materials, 24 (1980).
26. D.G. Kolman and J.R. Scully, *Journal of the Electrochemical Society*, 141, 2633 (1994).
27. J.E. Harrar, J.F. Carley, W.F. Isherwood, and E. Raber, *Report of the Committee to Review the Use of J-13 Well Water in Nevada Nuclear Waste Storage Investigations*, UCID-21867, Livermore, CA: Lawrence Livermore National Laboratory (1990).
28. R.W. Schutz and J.S. Grauman, *Laboratory corrosion behavior of titanium and other high performance alloys in representative FGD scrubber environments*, *Corrosion*/85, Paper no. 52, Houston, TX: NACE International (1985).
29. W. Wilhelmsen and A.P. Grande, *Electrochimica Acta*, 32, 1469 (1987).
30. M.J. Mandry and G. Rosenblatt, *Journal of the Electrochemical Society*, 119, 29 (1972).
31. V.A. Levin, *Zashchita Metallov*, 32, 143 (1996).
32. G. Kossyi, V.M. Novakovskii, and Ya.M. Kolotyarkin, *Zashchita Metallov*, 5, 210 (1969).

33. G. Boere, *Journal of Applied Biomaterials*, 6, 283 (1995).

TABLE 1

Composition of Ti Grade 7 base material, weld wire, and weldments used in the current study (wt%)

Material	C	Fe	N	O	H	Pd	Ti
Base Plate	0.019	0.115	0.007	0.140	0.005	0.15	bal.
Weld Wire	0.027	0.030	0.002	0.046	0.002	0.18	bal.
Weld Metal	0.026	0.080	0.005	0.100	0.003	0.16	bal.



## List of Figures

Figure 1: Potentiodynamic polarization curve for a creviced Ti Grade 7 specimen in deaerated 10 M LiCl solution at 95 °C.  $E_{bd}$ : breakdown potential;  $E_{rp}$ : repassivation potential. A potential scan rate of 0.167 mV/s was used.

Figure 2: Effect of chloride concentration on the breakdown potential and repassivation potential of wrought and welded Ti Grade 7 in deaerated NaCl solutions at 95 °C.

Figure 3: SEM micrograph of localized corrosion observed after potentiodynamic polarization of Ti Grade 7 in deaerated, 1 M NaCl at 95 °C. Note no attack was observed under the crevice former with all corrosion attack occurring on the boldly exposed surfaces.

Figure 4: Effect of temperature on the breakdown potential of wrought and welded Ti Grade 7 specimens in deaerated 1 and 4 M NaCl.

Figure 5: Effect of temperature on the repassivation potential of wrought and welded Ti Grade 7 specimens in deaerated 1 and 4 M NaCl.

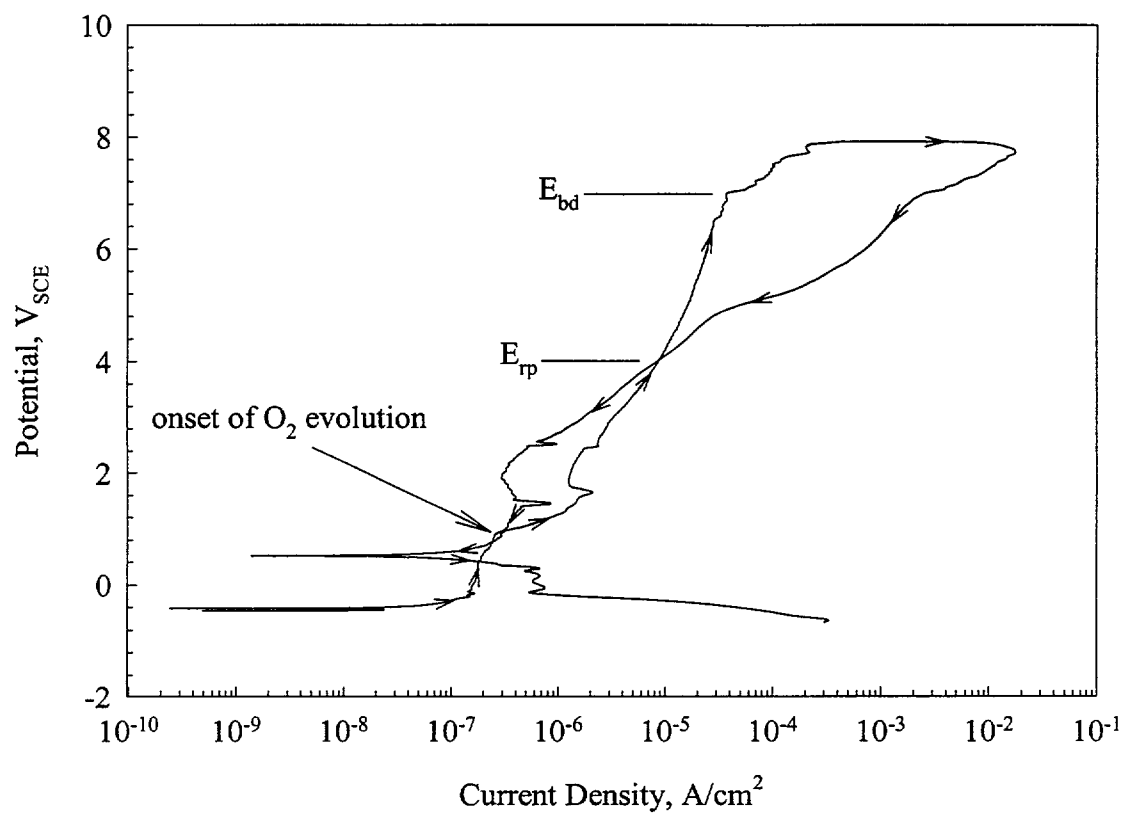
Figure 6: Effect of chloride concentration and applied potential on the short-term passive current density of Ti Grade 7 from 24 h potentiostatic polarization in deaerated solutions at 95 °C.

Figure 7: Effect of pH and applied potential on the short-term passive dissolution of Ti Grade 7 from 24 h potentiostatic polarization in deaerated 1 M chloride solutions at 95 °C.

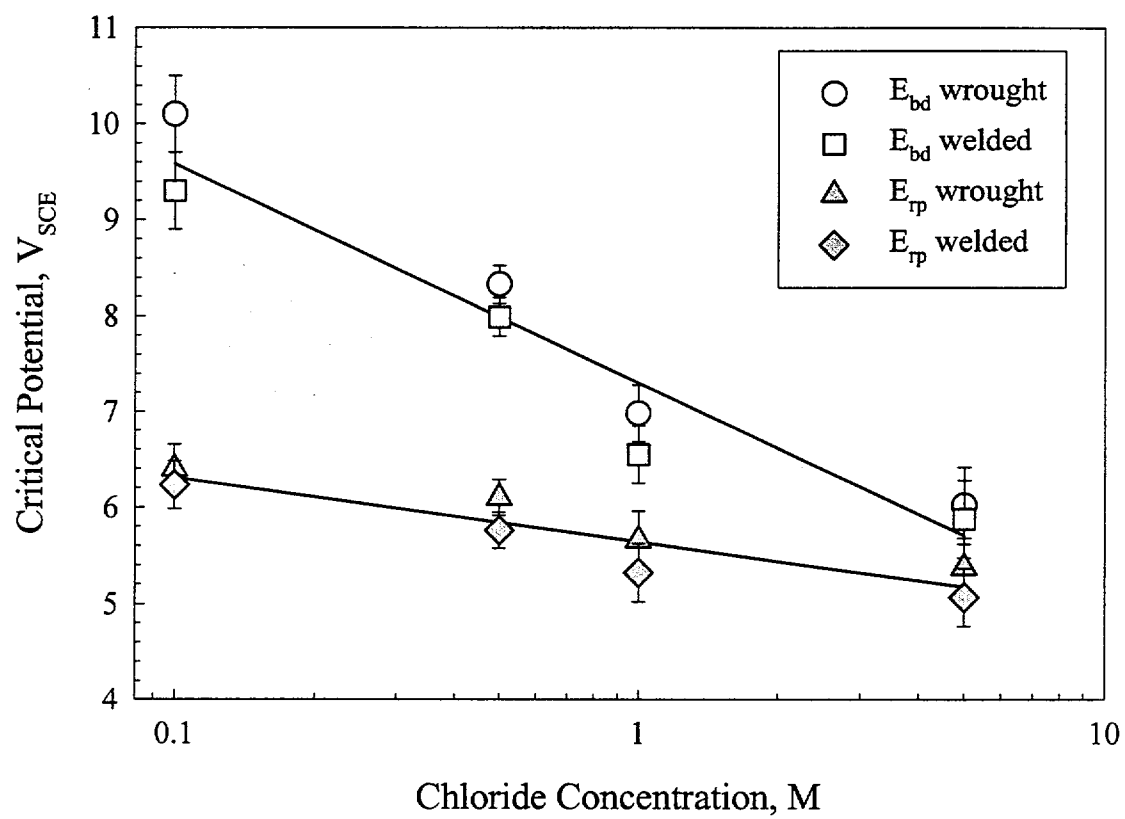
Figure 8: Passive current density of Ti Grade 7 in deaerated 1 M NaCl at 95 °C at an applied potential of 0 V<sub>SCE</sub> as a function of time out to ~ 1160 h (~ 7 wks).

Figure 9: Effect of fluoride on the anodic potentiodynamic polarization of Ti Grade 7 in deaerated solutions at 95 °C. Note that the horizontal lines at ~ 0 and ~ -0.3 V<sub>SCE</sub> bound the steady state open circuit potentials measured in air-saturated chloride solutions at 95 °C.

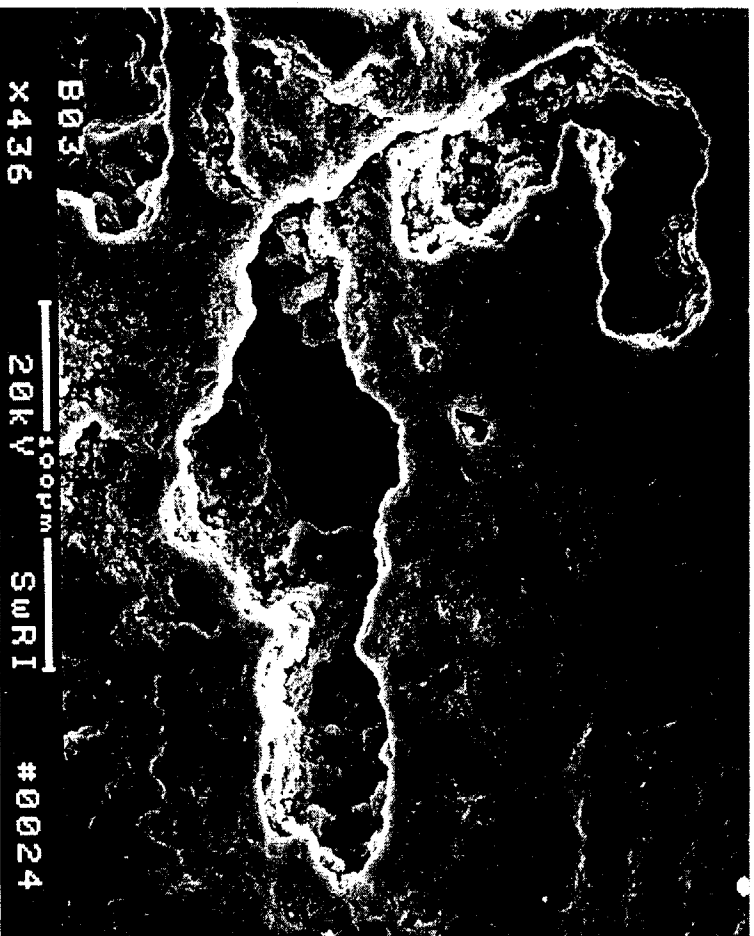
Figure 10: Effect of fluoride concentration on the passive current density measured at 0 V<sub>SCE</sub> from potentiodynamic polarization curves for both wrought and welded Ti Grade 7 specimens in deaerated 1 M NaCl at 95 °C and for wrought material in 0.1 M NaCl at 95 °C. For comparison, the current density in 1 M NaCl without fluoride is also shown.



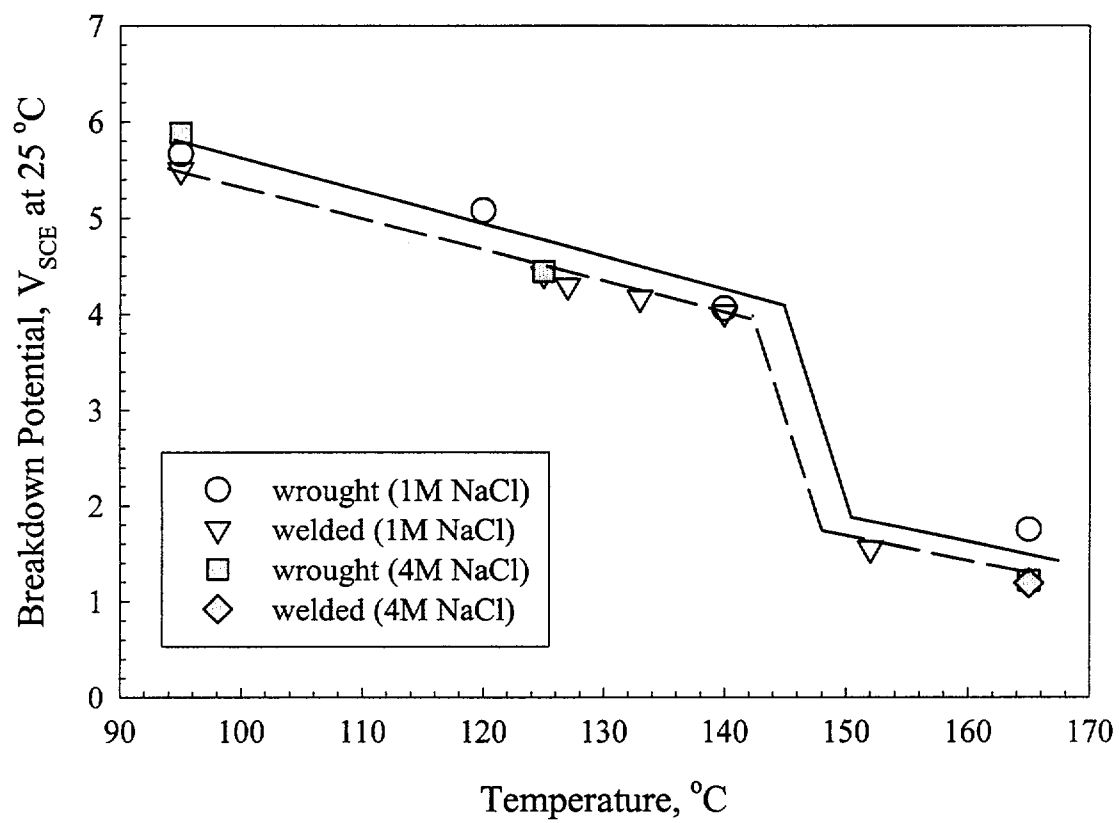
Brossia & Cragolino Figure 1



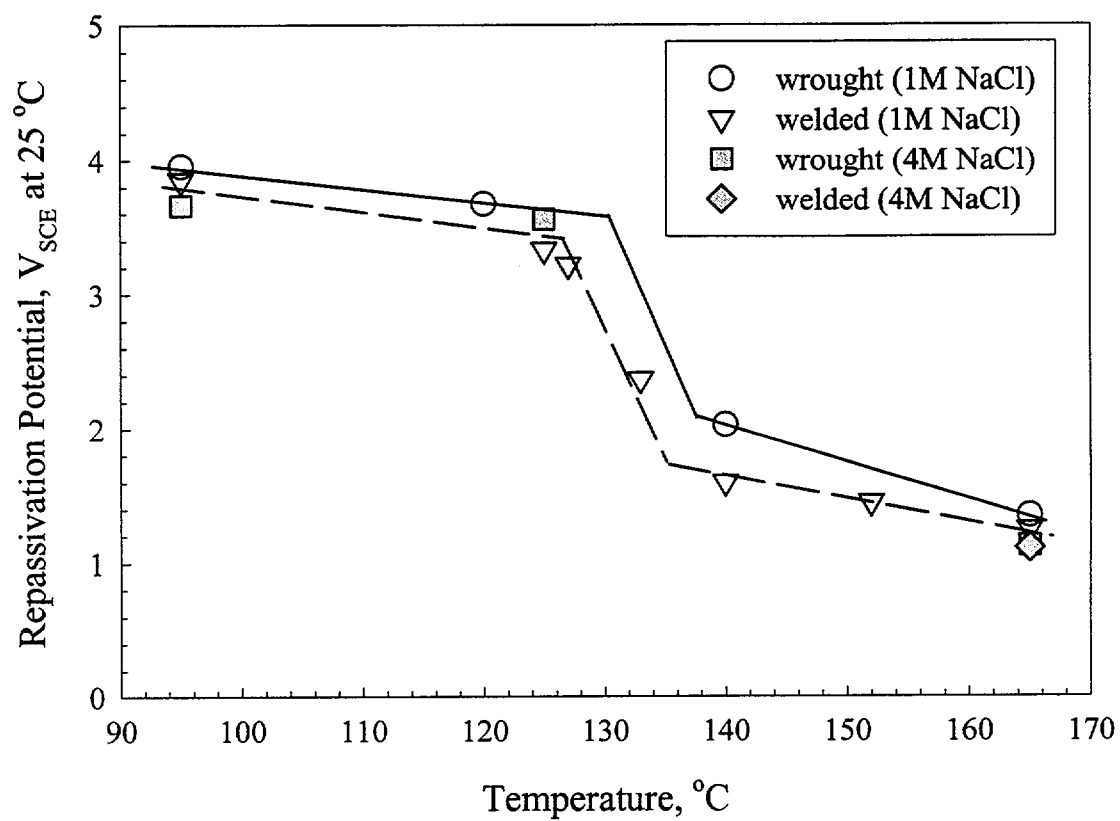
Brossia & Cragolino, Figure 2



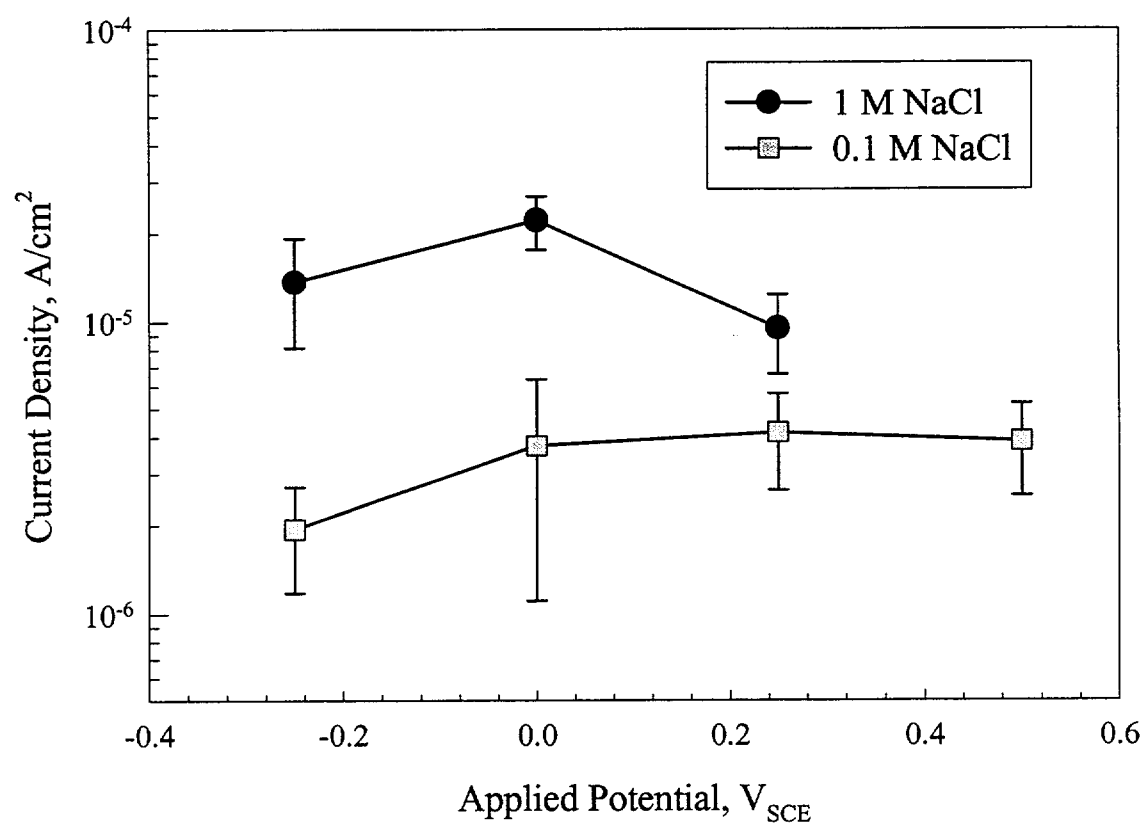
*Brossia* & *Craguoline*, Figure 3



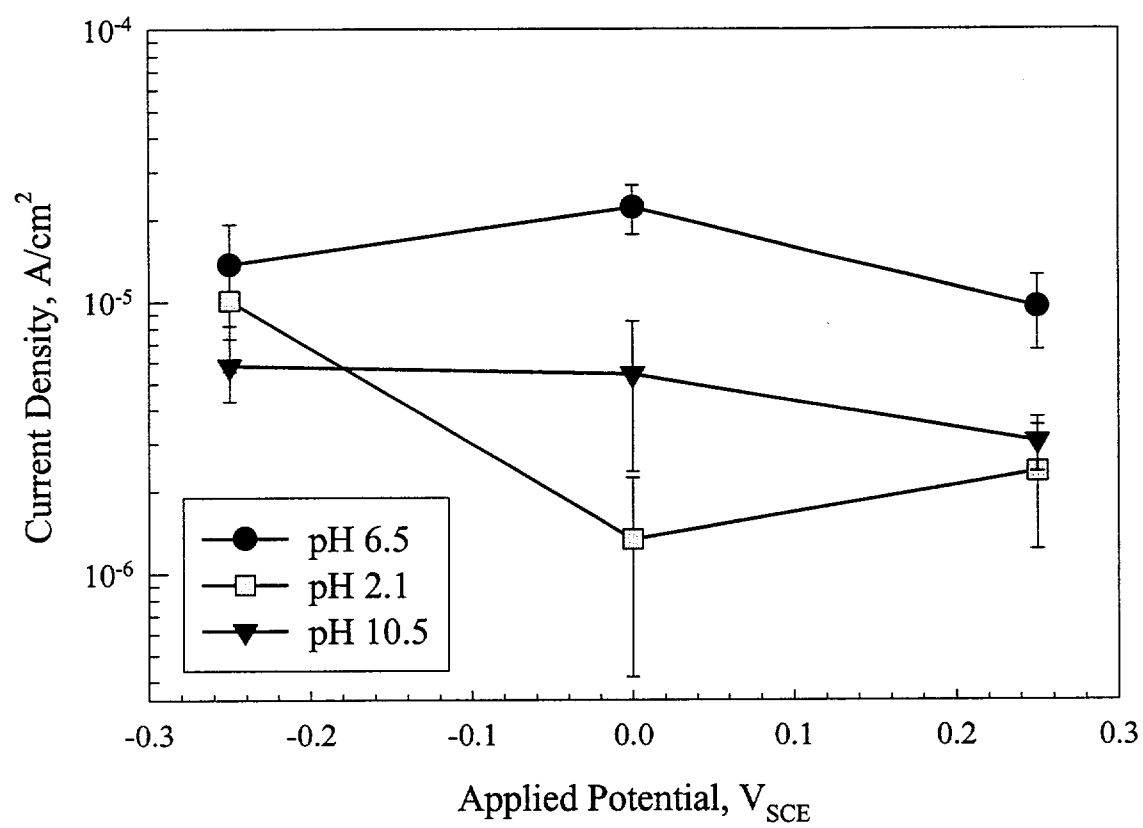
Brossia & Cragnolino, Figure 4



Brossie & Cragolino, Figure 5

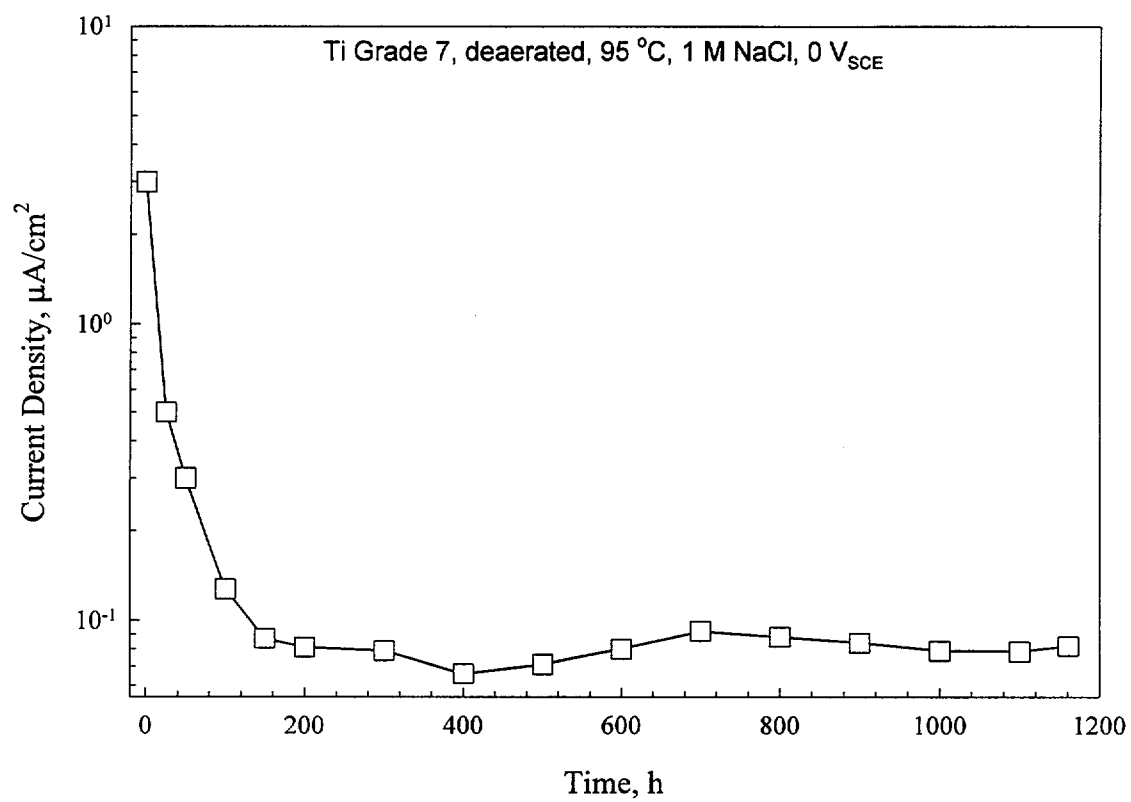


Brossia & Cragolino, Figure 6

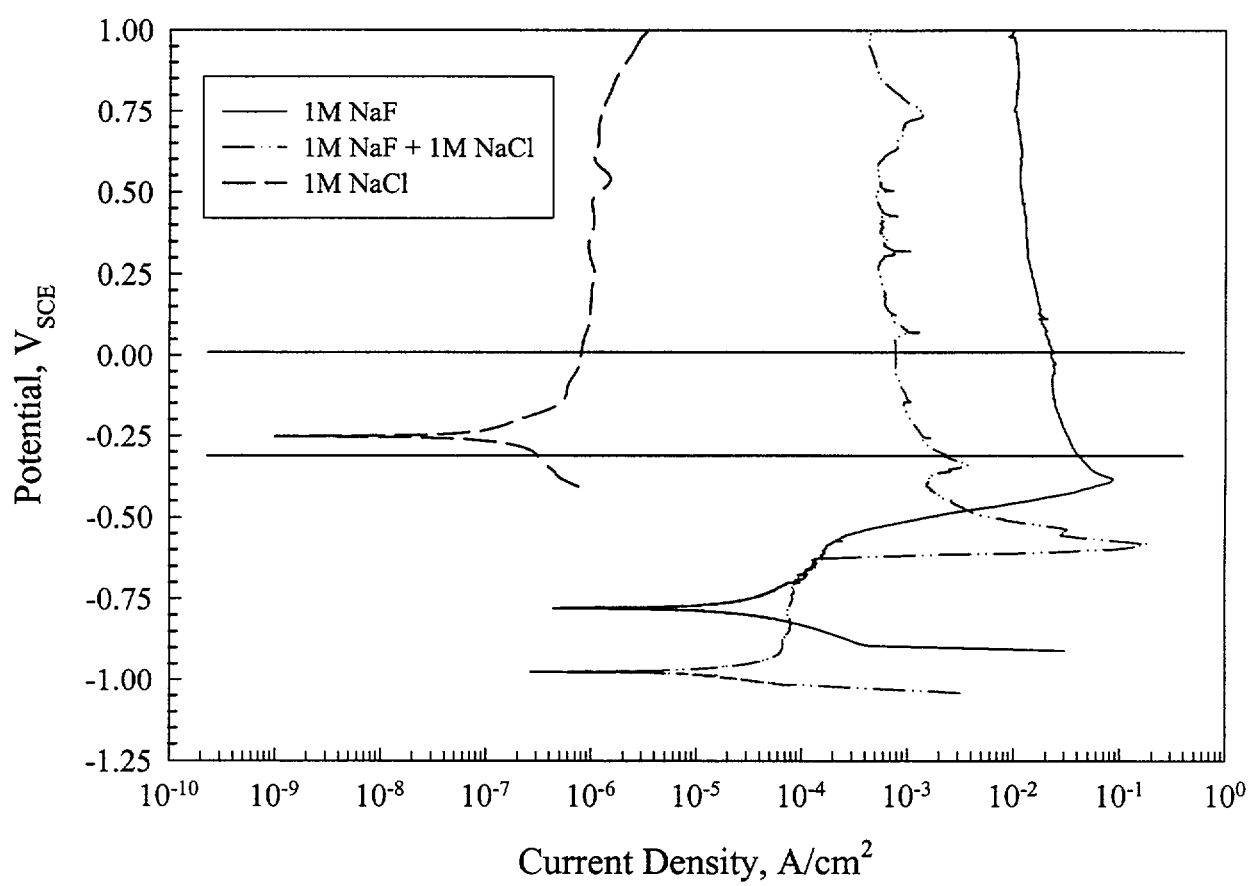


Porossia & Cragnolino, Figure 7

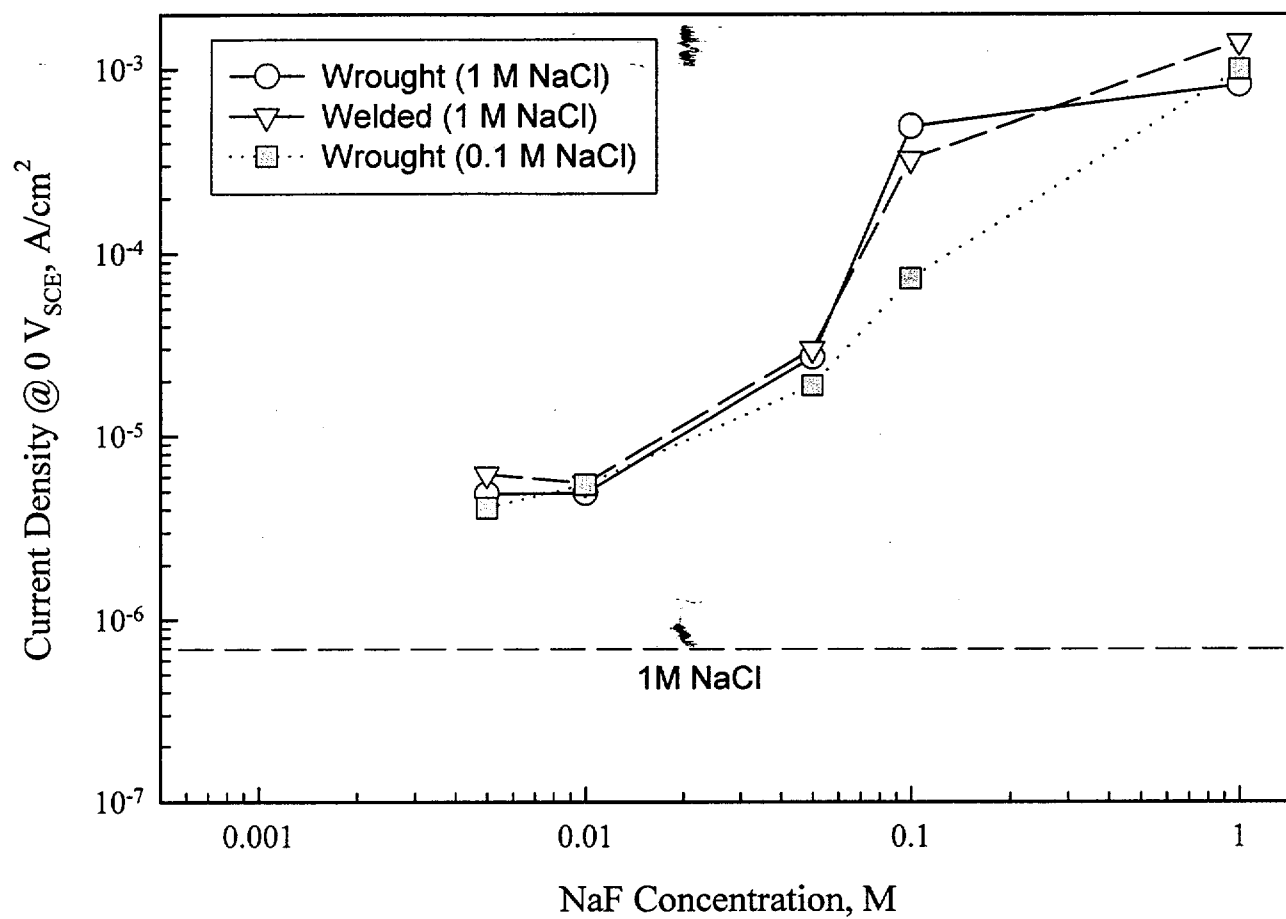




Brossia & Cragnolino, Figure 8



Brossia & Cragnolino, Figure 9



Porossia & Craynolds, Figure 10